

# Ninjurin1 Enhances the Basal Motility and Transendothelial Migration of Immune Cells by Inducing Protrusive Membrane Dynamics\*

Received for publication, March 26, 2014, and in revised form, June 9, 2014. Published, JBC Papers in Press, June 10, 2014, DOI 10.1074/jbc.M113.532358

Bum Ju Ahn<sup>‡</sup>, Hoang Le<sup>‡</sup>, Min Wook Shin<sup>‡</sup>, Sung-Jin Bae<sup>‡</sup>, Eun Ji Lee<sup>‡</sup>, Sung Yi Lee<sup>‡</sup>, Ju Hee Yang<sup>‡</sup>, Hee-Jun Wee<sup>‡</sup>, Jong-Ho Cha<sup>‡</sup>, Ji Hae Seo<sup>‡1</sup>, Hye Shin Lee<sup>‡</sup>, Hyo-Jong Lee<sup>‡5</sup>, Ken Arai<sup>¶</sup>, Eng H. Lo<sup>¶12</sup>, Sejin Jeon<sup>||</sup>, Goo Taeg Oh<sup>||3</sup>, Woo Jean Kim<sup>\*\*</sup>, Ji-Kan Ryu<sup>\*\*</sup>, Jun-Kyu Suh<sup>\*\*4</sup>, and Kyu-Won Kim<sup>‡††4,5</sup>

From the <sup>‡</sup>SNU-Harvard NeuroVascular Protection Research Center, College of Pharmacy and Research Institute of Pharmaceutical Sciences, Seoul National University, Seoul 151-742, Korea, the <sup>††</sup>Department of Molecular Medicine and Biopharmaceutical Sciences, Graduate School of Convergence Science and Technology, and College of Medicine or College of Pharmacy, Seoul National University, Seoul 151-742, Korea, the <sup>‡5</sup>College of Pharmacy, Inje University, Gimhae 621-749, Korea, the <sup>¶</sup>Neuroprotection Research Laboratory, Departments of Radiology and Neurology, Massachusetts General Hospital and Harvard Medical School, Boston, Massachusetts 02114, the <sup>||</sup>Department of Life Science and GT5 Program, Ewha Womans University, Seodaemun-gu, Seoul 120-750, Korea, and the <sup>\*\*</sup>National Research Center for Sexual Medicine and Department of Urology, Inha University School of Medicine, Incheon 402-751, Korea

**Background:** Ninjurin1 promotes leukocyte trafficking during inflammation through homotypic binding.

**Results:** Changes in Ninjurin1 expression in macrophages regulate protrusive membrane dynamics, motility, and in turn transendothelial migration.

**Conclusion:** The pro-migratory function and binding activity of Ninjurin1 are important for modulating immune responses during inflammation.

**Significance:** This study provides additional insights into the understanding of Ninjurin1-mediated inflammation.

Ninjurin1 is involved in the pathogenesis of experimental autoimmune encephalomyelitis, an animal model of multiple sclerosis, by mediating leukocyte extravasation, a process that depends on homotypic binding. However, the precise regulatory mechanisms of Ninjurin1 during inflammation are largely undefined. We therefore examined the pro-migratory function of Ninjurin1 and its regulatory mechanisms in macrophages. Interestingly, Ninjurin1-deficient bone marrow-derived macrophages exhibited reduced membrane protrusion formation and dynamics, resulting in the impairment of cell motility. Furthermore, exogenous Ninjurin1 was distributed at the membrane of filopodial structures in Raw264.7 macrophage cells. In Raw264.7 cells, RNA interference of Ninjurin1 reduced the number of filopodial projections, whereas overexpression of Ninjurin1 facilitated their formation and thus promoted cell

motility. Ninjurin1-induced filopodial protrusion formation required the activation of Rac1. In Raw264.7 cells penetrating an MBEC4 endothelial cell monolayer, Ninjurin1 was localized to the membrane of protrusions and promoted their formation, suggesting that Ninjurin1-induced protrusive activity contributed to transendothelial migration. Taking these data together, we conclude that Ninjurin1 enhances macrophage motility and consequent extravasation of immune cells through the regulation of protrusive membrane dynamics. We expect these findings to provide insight into the understanding of immune responses mediated by Ninjurin1.

Rapid movement of immune cells toward an inflammatory region is an essential prerequisite for the initiation of their sequential functions (1). Myeloid-lineage immune cells such as resident macrophages and sentinel circulating monocytes are always ready for an emergency, providing high level surveillance by finding the signals of danger and quickly migrating toward infected or damaged sites (2, 3). These recruited myeloid cells can function as a major regulator of innate immunity by mediating cytokine release, phagocytosis, and the resolution of inflammation, as well as alerting additional adaptive immunity by priming the activation of T lymphocytes. Therefore, understanding macrophage movement during inflammation is an interesting and important area of research (4).

Macrophages use an amoeboid migration mechanism that differs greatly from that of slow moving fibroblasts and epithelial cells. Amoeboid migration involves weak adhesive interactions with the surrounding environmental substrate and generates fast sliding-type movements in tissues (5, 6). During

\* This work was supported by a grant from a National Research Foundation of Korea, a grant funded by the Ministry of Education, Science and Technology through the Global Research Laboratory Program (2011-0021874), Brain Korea 21 Program, and the Global Core Research Center Program Grant 2012-0001187.

<sup>1</sup> Supported by Basic Science Research Program through the National Research Foundation funded by Ministry of Education, Science and Technology Grant 2013R1A1A2058956.

<sup>2</sup> Supported by National Institutes of Health Grants R37-NS37074, R01-76694, and P01-NS55104 (to E. H. L.).

<sup>3</sup> Supported by National Research Foundation Grant 2013003407 funded by the Korean Government (Ministry of Education, Science and Technology).

<sup>4</sup> Supported by Korea Healthcare Technology R&D Project, Ministry for Health, Welfare and Family Affairs Grant A110076.

<sup>5</sup> To whom correspondence should be addressed: SNU-Harvard NeuroVascular Protection Research Center, College of Pharmacy and Research Institute of Pharmaceutical Sciences, Seoul National University, Seoul 151-742, Korea. Tel.: 82-2-880-6988; Fax: 82-2-885-1827; E-mail: qwonkim@snu.ac.kr.

macrophage migration, the membrane extension event (*i.e.* protrusion formation) at the leading edge is essential for general cell motility (7). Because the contribution of adhesive interaction with substrates during amoeboid migration is less important for movement, the protrusive membrane activity in macrophages is thought to be the major driving force of their migration.

Macrophages can generate broad pseudopodia and spike-like filopodia in the direction of a chemotactic gradient in response to migratory cues (8, 9). These protrusive structures are dynamically regulated by the components of the cytoskeleton and cytoplasmic signaling. F-actin polymerization is tightly controlled at the leading edge, which is defined by the protrusive membrane to determine the direction of movement. In the cytoplasm of moving cells, the Rho family of small GTPases, including RhoA, Rac1, and Cdc42, mediate the signal from the plasma membrane to regulate actin reorganization during the macrophage migration process (10–13).

Ninjurin1 is a small size transmembrane adhesion molecule containing 152 amino acids (~17 kDa). Ninjurin1 includes an N-terminal (amino acids 1–71) and C-terminal (amino acids 139–152) ectodomain, two transmembrane domains (amino acids 72–100 and 111–138), and an intercellular region (amino acids 101–110). Through the homophilic binding domain (amino acids 26–37) of its N-terminal ectodomain, Ninjurin1 binds with itself. Ninjurin1 was originally identified in the neurons and Schwann cells of the peripheral nervous system, where it induces neurite extension (14, 15). Some studies have revealed the role of Ninjurin1 in the immune pathogenesis of multiple sclerosis (MS)<sup>6</sup> and its animal model, experimental autoimmune encephalomyelitis (EAE) (16–18). Highly migratory T cells were recently reported to be active in the lungs of EAE rats, and Ninjurin1 was found to be transiently up-regulated and involved in the intravascular crawling of T cells in central nervous system vessels (19), indicating the involvement of Ninjurin1 in the motility of T cells. However, Ninjurin1 expression is predominantly in myeloid cells rather than lymphoid cells. Moreover, its additional functions beyond homophilic binding during inflammation are largely unknown.

Here, we investigated the role of Ninjurin1 in macrophage motility. Intriguingly, Ninjurin1 facilitates the migration of bone marrow-derived macrophages (BMDMs) and Raw264.7 cells through the regulation of protrusive membrane dynamics. Moreover, Ninjurin1-mediated membrane protrusion formation relies on the activation of Rac1. Taken together, our data show a novel function of Ninjurin1 in macrophage locomotion under inflammatory conditions in addition to its well known homophilic binding activity.

## EXPERIMENTAL PROCEDURES

**Animals**—Ninjurin1 KO mice (C57BL/6J background) were generated by removing exon 1 of the four exons encoding Ninjurin1 located on chromosome 13 using homologous recombination. These mice were backcrossed with C57BL/6 for at least

seven generations. The breeding colony was maintained under pathogen-free conditions in the animal housing facility of the College of Pharmacy, Seoul National University, for the duration of the experiments. We adhered to the rules of the Committee for Care and Use of Laboratory Animals at Seoul National University (SNU-101011-1). The following primer sequences were used for genotyping: wild type (forward), 5'-GAG ATA GAG GGA GCA CGA CG-3'; Neo (forward), 5'-ACG CGT CAC CTT AAT ATG CG-3', and reverse primer, 5'-CGG GTT GTT GAG GTC ATA CTT G-3'.

**Cell Culture**—Raw264.7 and mouse brain endothelial cell 4 (MBEC4) cells were grown in Dulbecco's modified Eagle's medium (Invitrogen) supplemented with 10% fetal bovine serum (FBS, Invitrogen) and maintained in an incubator with a humidified atmosphere of 95% O<sub>2</sub> and 5% CO<sub>2</sub> at 37 °C. For the BMDM culture, bone marrow cells were obtained from the femurs and tibias of mice (C57BL/6J) at 6–10 weeks of age and were cultured in RPMI 1640 medium containing 10% FBS and 1% penicillin and streptomycin for 3 days. Cells were differentiated in RPMI 1640 medium containing 20 ng/ml macrophage-colony stimulating factor (PeproTech) for 3 days.

**Antibodies**—To generate the custom-made anti-mouse Ninjurin1 antibody, a keyhole limpet hemocyanin-conjugated synthetic peptide containing mouse Ninjurin1 residues 1–15 (Ab<sub>1–15</sub>) was immunized into rabbits following standard procedures (Peptron Inc. and Abfrontier Inc., Korea) as described previously (20). Anti-Ninjurin1 antibodies were purified using antigen-specific affinity chromatography. Immunostaining and Western blotting were performed using Ab<sub>1–15</sub>.

**Time-lapse Imaging**—Time-lapse series of the BMDMs and Raw264.7 cells were taken at 37 °C using microscopes (Carl Zeiss, Axiovert M200 and LSM 700) equipped with computer-driven cooled CCD cameras, humidified CO<sub>2</sub> chambers, and autofocus systems. We used the Axiovert M200 microscope to image cell motility and LSM700 to image membrane dynamics.

**Construction of the Expression Vectors and Stable Raw264.7 Cell Line**—The full-length cDNA sequence encoding the human Fascin1 protein (BC000521) was cloned into the pTagRFP-C (Evrogen) backbone plasmid. pCS2<sup>+</sup> Myc tag Ninjurin1 vectors (Myc-mNinj1) were transfected to overexpress Ninjurin1 in Raw264.7 cells (Nucleofector, Amaxa), as described previously (21). To construct stable Ninjurin1-overexpressing Raw264.7 cells, full-length cDNA encoding mouse Ninjurin1 (NM\_013610) was cloned into the pEGFP C3 backbone plasmid (Clontech, GFP-mNinj1). The GFP-mNinj1 plasmid was transfected into Raw264.7 cells and incubated in complete Dulbecco's modified Eagle's medium containing G418 (500 μg/ml). After several days, the existing colonies were selected. Purity and homogeneity (>90%) were estimated using fluorescent microscope observations and Western blotting.

**RNA Interference**—For RNA interference (RNAi) knock-down of Ninjurin1 in Raw264.7 cells, small interfering RNAs (siRNAs) that target mouse Ninjurin1 (NM\_013610; siNinj1) were purchased from Invitrogen. Negative control siRNAs (siCont) were pre-designed by Bioneer Inc. (Korea). The siRNA sequences were as follows: siCont, 5'-CCT ACG CCA CCA AUU UCG U dTdT-3', and siNinj1, 5'-ACC GGC CCA UCA AUG UAA ACC AUU A-3'. Using Nucleofector (Amaxa), each

<sup>6</sup>The abbreviations used are: MS, multiple sclerosis; BMDM, bone marrow-derived macrophage; EAE, experimental autoimmune encephalomyelitis; TEM, transendothelial migration.

## Ninjurin1-mediated Motility in Immune Cells

siRNA was transfected into Raw264.7 cells at a concentration <200 pmol/sample. The Ninjurin1 knockdown efficiency was determined by Western blotting using anti-green fluorescent protein (GFP) and anti-Ninjurin1 (Ab<sub>1-15</sub>) antibodies.

**Quantification of Filopodial Membrane Protrusions in Raw264.7 Cells**—To quantify the number of filopodia in Raw264.7 cells, RFP-Fascin1 was transfected into the stable cell line or co-transfected with siRNA. After 24 h, the number of filopodia expressing RFP-Fascin1 per cell was quantified. Raw264.7 cells were plated on MBEC4 monolayers. The Raw264.7 cells that were transfected with RFP-Fascin1 or siRNA were incubated for 15 min on a MBEC4 monolayer that had been stimulated with 10 ng/ml tumor necrosis factor  $\alpha$  (TNF $\alpha$ ) and 10 ng/ml interferon- $\gamma$  (IFN- $\gamma$ ) for 16 h. After fixation, RFP-Fascin1-expressing filopodia of the Raw264.7 cells were counted. To evaluate the distribution of Ninjurin1 in cells during the transendothelial migration (TEM) assay, Raw264.7 cells transfected with Myc-mNinj1 were added to a carboxy-fluorescein diacetate succinimidyl ester-labeled MBEC4 monolayer. After 20 min of incubation, the samples were fixed in 4% paraformaldehyde and stained using anti-Myc antibody (Santa Cruz Biotechnology).

**Cell Adhesion and Spreading Assays**—To measure the adhesion and spreading activity of overexpressing or siRNA Raw264.7 cells, the cells ( $3 \times 10^5$ ) were added to cover glass (12 mm, Marienfeld) coated with fibronectin (50  $\mu$ g/ml) and incubated for 15 min. After washing three times with PBS, the cells were fixed with 4% paraformaldehyde. The adherent cells were imaged in at least six positions by microscopy. The number of adherent cells and their area of spreading were measured using ImageJ software (National Institutes of Health), and values were normalized to that of control cells. In the siRNA Raw264.7 cells, interferon- $\gamma$  (INF- $\gamma$ ) (10 ng/ml, 16 h)-stimulated cells were used to measure the difference in cell spreading.

**Immunoblotting**—Proteins were extracted using a cell lysis buffer containing 20 mM Tris-HCl (pH 7.5), 150 mM NaCl, 1 mM Na<sub>2</sub>EDTA, 1 mM EGTA, 1% Triton X-100, 2.5 mM sodium pyrophosphate, 1 mM  $\beta$ -glycerophosphate, 1 mM Na<sub>3</sub>VO<sub>4</sub>, 1  $\mu$ g/ml leupeptin, and a protease inhibitor mixture. After one-dimensional SDS-PAGE, membranes were immunoblotted using anti-Ninjurin1 (Ab<sub>1-15</sub>), anti-GFP (Abcam), and anti-actin (Sigma) primary antibodies overnight at 4 °C. HRP-conjugated secondary antibodies were incubated with the membranes for 1 h at room temperature. Visualization was performed using ECL Plus (iNtRON) and LAS-4000 (GE Healthcare). Actin was used as an internal loading control.

**RT-PCR**—Total RNA from the stable GFP Raw264.7 cell line was purified using TRIzol (Invitrogen). RT-PCR analysis was performed as described previously (21). The following primers were used for RT-PCR: *Gapdh*, sense 5'-ACC ACA GTC CAT GCC ATC AC-3' and antisense 5'-TCC ACC ACC CTG TTG CTG TA-3'; *Ninj1*, sense 5'-TGA GGA GTA TGA GCT CAA CG-3' and antisense 5'-GAT GTC CAG CAT GCT CTC CGC-3'.

**Immunofluorescence Staining and Microscopy**—Cells were incubated with anti-F4/80 (Serotec), anti-Myc, and Alexa 546 phalloidin (Molecular Probes). After incubation with primary antibodies (overnight at 4 °C), cells were stained using Alexa

488-conjugated IgG or Alexa 546-conjugated IgG (Molecular Probes) secondary antibodies for 1 h at room temperature. Nuclei staining was performed using Hoechst 33342 (Molecular Probes). Both Axiovert M200 and LSM 700 microscopes were used for immunofluorescence imaging.

**Small GTPase Activity and Inhibitors**—We analyzed the activity of small GTPases in the BMDMs and Raw264.7 cells by using the recommended procedure provided with the G-LISA Assay Biochem kit (Cytoskeleton Inc.). The activities of RhoA (BK124), Rac (BK125), and Cdc42 (BK127) were assessed. For the pharmacological inhibition study, GFP-mNinj1 Raw264.7 cells were treated with either NSC23766 (Rac1 inhibitor, Tocris) or the dimethyl sulfoxide carrier for 3 h at the indicated concentrations.

**Data Analysis and Statistics**—All data are presented as the means  $\pm$  S.E. Statistical significance was evaluated using an unpaired two-tailed Student's *t* test for single comparisons. Asterisk indicates that *p* < 0.05 was considered statistically significant.

## RESULTS

**Cell Motility and Protrusive Membrane Dynamics Are Reduced in Ninjurin1-deficient BMDMs**—To analyze the function of Ninjurin1 in the migratory behavior of immune cells, we established primary BMDMs and raised an antibody (Ab<sub>1-15</sub>) to detect Ninjurin1 as described under "Experimental Procedures." Immunostaining was performed using the anti-F4/80 antibody, a macrophage-specific marker. Staining showed the high purity (>90%) of our BMDM cultures (Fig. 1A). Western blots performed using Ab<sub>1-15</sub> on wild-type (WT) or Ninjurin1-deficient BMDM cell lysates revealed the specificity of this antibody for mouse Ninjurin1 (Fig. 1B). We examined the basal motility of WT and Ninjurin1-deficient BMDMs. The time-lapse analysis performed under lower magnification microscopy showed that the Ninjurin1-deficient BMDMs had reduced motility (Fig. 1C), with a lower velocity and shorter Euclidean distance compared with WT BMDMs (Fig. 1D), providing evidence that Ninjurin1 contributes to basal motility in BMDMs.

Membrane protrusions such as pseudopodia and filopodia at the leading edge are necessary for cell movement (22). Because Ninjurin1 is involved in cell migration (Fig. 1, C and D), we evaluated the protrusive activity of WT and Ninjurin1-deficient BMDMs by drawing difference plots of their boundaries in successive video frames (Fig. 2A). WT BMDMs were found to generate active pseudopodial membrane extensions and move faster than Ninjurin1-deficient cells (Fig. 2A). Next, we analyzed the F-actin intensity of WT and Ninjurin1-deficient BMDMs in the whole cell area via phalloidin staining. The fluorescence intensity of Alexa 546 phalloidin staining was stronger in WT BMDMs than in the Ninjurin1-deficient cells (Fig. 2, B and C). In addition, the WT BMDMs showed a concentrated pattern of phalloidin staining at the leading edge, although Ninjurin1-deficient cells had diffuse staining (Fig. 2B), indicating higher protrusive activity in WT BMDMs than in Ninjurin1-deficient cells. Because membrane dynamics are also important in cell migration, we examined membrane ruffling in WT and Ninjurin1-deficient BMDMs by using high magnification time-lapse microscopy. Ninjurin1-deficient BMDMs had fewer

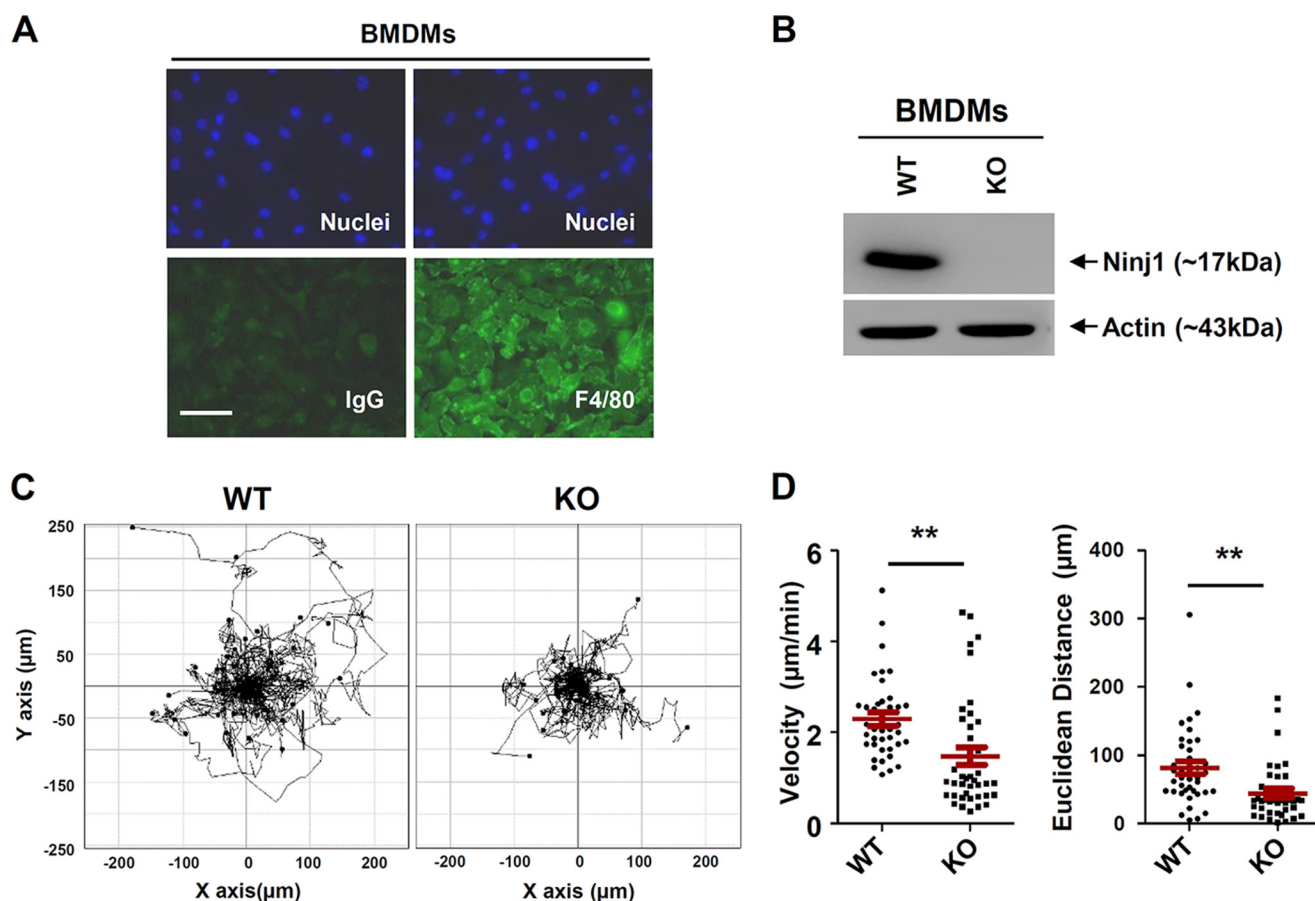


**FIGURE 1. Ninjurin1 deficiency decreases motility of bone marrow-derived macrophages.** *A*, BMDMs isolated from wild-type (*WT*) mice were cultured and then immunostained using an antibody against F4/80 (green), a macrophage marker, or an IgG control. The nuclei of BMDMs were counterstained using Hoechst 33342 (blue). Scale bar, 50  $\mu\text{m}$ . *B*, WT and Ninjurin1-deficient BMDMs were subjected to Western blot analysis performed using anti-Ninjurin1 antibody (Ab<sub>1-15</sub>). *C* and *D*, basal motility of WT and Ninjurin1-deficient BMDMs. Images of WT and Ninjurin1-deficient BMDMs were obtained every 10 min for 6 h on the uncoated surface of a six-well plate. Trajectory plot (*C*) and dot charts (*D*) show the velocity and Euclidean distance of 40 cells. \*\*,  $p < 0.01$ .

membrane ruffles (Fig. 2*D*) and a smaller difference in the changed cell area at the set time interval (Fig. 2, *D* and *E*) than that in the case of WT cells. These data suggest that Ninjurin1 is required for membrane dynamics and subsequent basal motility in BMDMs.

**Localization of Ninjurin1 to Filopodial Membrane Structures**—To examine the subcellular distribution of Ninjurin1, we overexpressed GFP-mNinj1 in BMDMs. The overexpressed GFP-mNinj1 localized to slender membrane protrusions that we assumed to be filopodia (Fig. 3*A*). Indeed, the transfected GFP-mNinj1 signals in Raw264.7 cells co-localized with a filopodial marker, RFP-Fascin1 (Fig. 3*B*), and Alexa 546 phalloidin staining (Fig. 3*C*). Therefore, these results indicate that Ninjurin1 localizes to filopodial membrane structures, suggesting that Ninjurin1 contributes to their formation.

**Ninjurin1 Knockdown in Raw264.7 Cells by Using RNAi Leads to Fewer and Less Dynamic Filopodial Protrusions**—To examine the effects of Ninjurin1 on the formation of filopodial protrusions, we examined the projection properties of the Raw264.7 cells treated with Ninjurin1 RNAi (siNinj1). Western blots performed using Ab<sub>1-15</sub> (Fig. 4*A*) showed the efficiency of Ninjurin1 knockdown in cells treated with siNinj1 compared with those treated with the RNAi negative control (siCont). Interestingly, siNinj1 Raw264.7 cells had fewer filopodia

expressing the RFP-Fascin1 protein than the siCont cells (Fig. 4, *B* and *C*). In time-lapse imaging, siNinj1 Raw264.7 cells had fewer filopodium-like protrusions with less active protrusion dynamics than siCont Raw264.7 cells (Fig. 4*D*). In addition, we observed active random movement of cell bodies and small pseudopodial membrane extensions in siCont Raw264.7 cells (Fig. 4*D*). The number of cells attached to the fibronectin-coated plates and their spreading area of siNinj1 Raw264.7 cells were significantly decreased when compared with the siCont cells (Fig. 4, *E* and *F*), implying that the alteration of Ninjurin1-mediated cortical activity might be responsible for the extension of small pseudopodia. Taken together, these results demonstrate that the loss of Ninjurin1 in Raw264.7 cells reduces filopodial projections and disrupts their dynamics.

**Overexpression of Ninjurin1 in Raw264.7 Cells Enhances Cell Motility, Filopodial Protrusion Formation, and Protrusion Dynamics**—To directly address whether overexpressed Ninjurin1 enhances the migration of Raw264.7 cells, we generated stable Raw264.7 cell lines that constitutively express GFP or GFP-mNinj1. Western blots (Fig. 5*A*, top panel) validated the molecular mass (~44 kDa), and PCR (Fig. 5*A*, bottom panel) showed that Ninjurin1 mRNA expression in GFP-mNinj1 Raw264.7 cells was around 2.5-fold higher than that in GFP control cells. The results indicate the successful construction of

## Ninjurin1-mediated Motility in Immune Cells

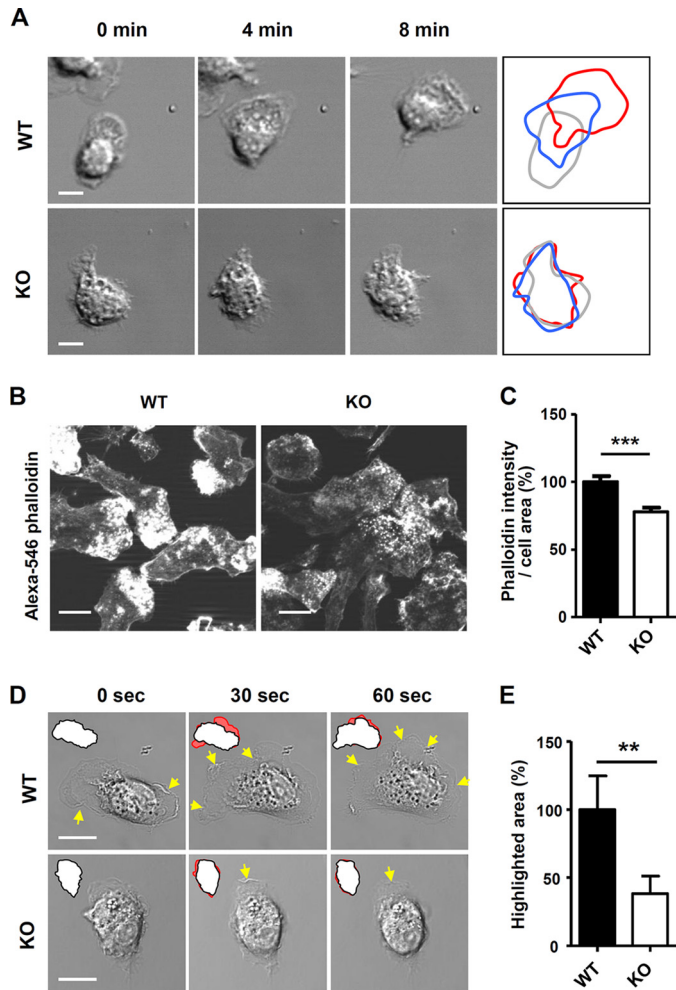


**FIGURE 2. Ninjurin1-deficient BMDMs have reduced membrane protrusions and less active dynamics.** *A*, differential plots of WT or Ninjurin1 knock-out (KO) BMDM cell boundaries from successive video frames. Scale bar, 10  $\mu\text{m}$ . *B* and *C*, Alexa 546 phalloidin staining of WT and KO BMDMs. Images were acquired using the same exposure times (*B*). The phalloidin intensity and area of each cell were measured using ImageJ software, and the values are expressed as the unit of intensity per area (*C*). Representative results are shown from three experiments. Scale bar, 10  $\mu\text{m}$ . **\*\*\***,  $p < 0.001$ . *D* and *E*, membrane dynamics of WT and Ninjurin1-deficient BMDMs. *D*, yellow arrows indicate the regions of membrane ruffling, and red highlighted regions indicate the differential cell area at each time point from successive video frames. *E*, highlighted area from ~20 cells per group was measured and normalized to that of WT cells. Scale bar, 10  $\mu\text{m}$ . **\*\***,  $p < 0.01$ .

the stable GFP and GFP-mNin1 Raw264.7 cell lines. Consistent with the results obtained for siNin1 Raw264.7 cells, the number of filopodia labeled with RFP-Fascin1 was increased in the GFP-mNin1 Raw264.7 cells compared with the GFP control (Fig. 5, *B* and *C*). To compare their membrane protrusion dynamics, high magnification time-lapse imaging of the stable GFP- or GFP-mNin1 Raw264.7 cell lines was performed. As expected, the stable GFP-mNin1 Raw264.7 cells showed random movements of their cell bodies and dynamic filopodial protrusions, and they generated pseudopodia-like feet (Fig. 5*D*). Consistent with the results of siRNA experiments, GFP-mNin1 Raw264.7 cells showed increased cell adhesion and spreading compared with that in the case of GFP cells alone (Fig. 5, *E* and *F*). To examine the basal motility of the

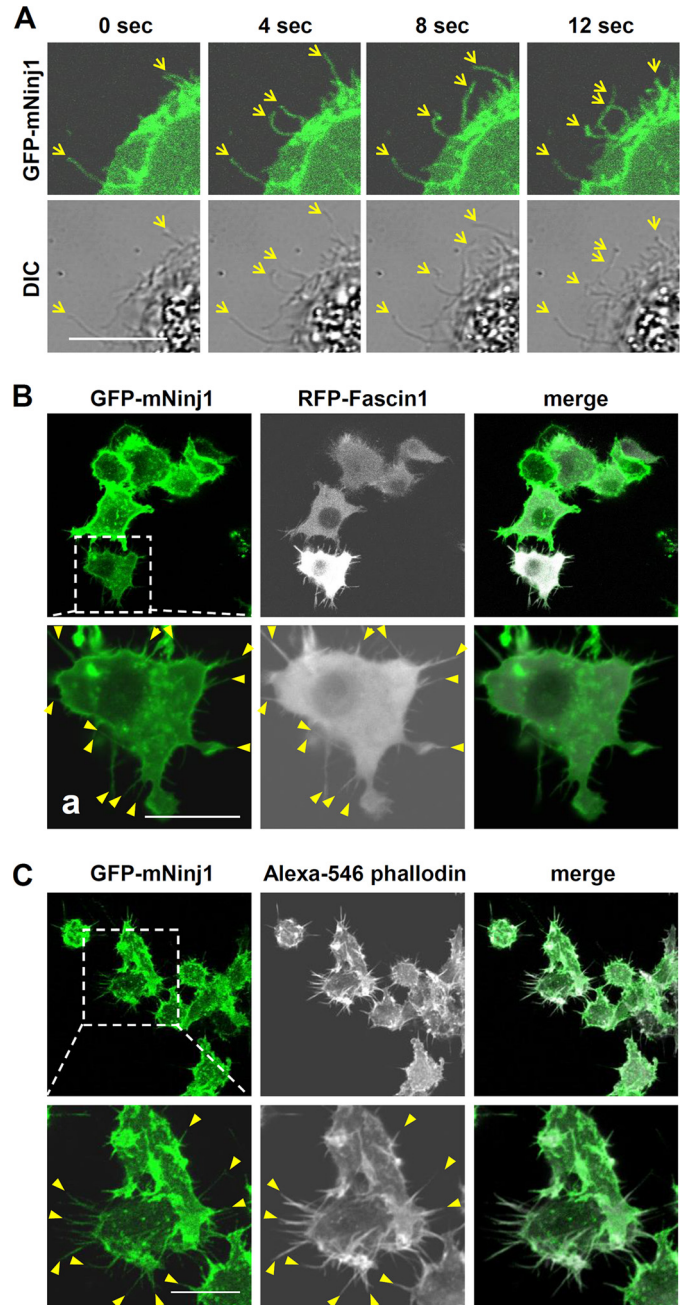


**FIGURE 3. Localization of GFP-mNin1 in filopodial structures.** *A*, distribution of GFP-mNin1 in BMDMs. Differential interference contrast (DIC) and GFP-mNin1 signals (green) were acquired at each time point by using confocal microscopy. Yellow arrows indicate filopodium-like structures. Scale bar, 10  $\mu\text{m}$ . *B* and *C*, co-localization of GFP-mNin1 with filopodial markers RFP-Fascin1 (*B*) and Alexa 546 phalloidin (*C*) in Raw264.7 cells. Square boxes show high magnification images of each labeled Raw264.7 cell, and yellow arrowheads indicate filopodial structures expressing RFP-Fascin1 (*B*) or Alexa 546-phalloidin (*C*). Scale bar, 10  $\mu\text{m}$ .

stable Raw264.7 cell lines, time-lapse imaging was performed under a low magnification microscope. GFP-mNin1 Raw264.7 cells showed increased motility (Fig. 6*A*), with a higher velocity and longer Euclidean distance compared with GFP control cells (Fig. 6*B*). Taken together, these data showed that overexpressed Ninjurin1 enhances the formation and dynamics of filopodial membrane protrusions to promote cell motility and movement.

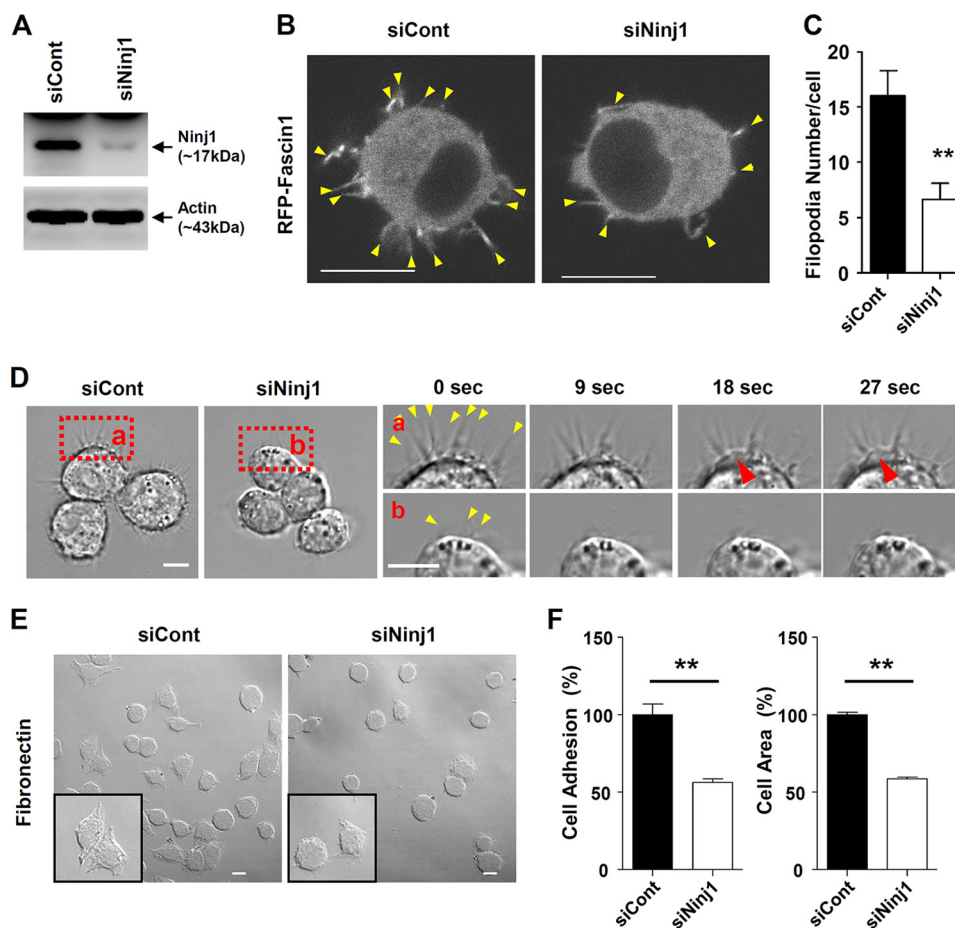


**FIGURE 4. Small interfering RNAs against Ninjurin1 decrease the formation of filopodial membrane protrusions in Raw264.7 cells.** *A*, Western blot analysis of Raw264.7 cells transfected with control (*siCont*) and Ninjurin1 (*siNinj1*) small interfering RNAs performed using the Ab<sub>1-15</sub> antibody. *B* and *C*, co-transfection of RFP-Fascin1 with *siCont* or *siNinj1* into Raw264.7 cells. Yellow arrowheads indicate filopodial structures expressing RFP-Fascin1 (*B*). The statistical data (*C*) were generated from the results of ~30 cells. Scale bar = 10  $\mu\text{m}$ . \*\*,  $p < 0.01$ . *D*, membrane dynamics of *siCont* and *siNinj1* Raw264.7 cells. The red squares (*a* and *b*) show high magnification images of *siCont* and *siNinj1* Raw264.7 cells, respectively. The red arrowheads show a small pseudopodia, and the yellow arrowhead shows filopodial protrusions. Scale bar, 10  $\mu\text{m}$ . *E* and *F*, adhesion and spreading of *siCont* and *siNinj1* Raw264.7 cells stimulated with interferon- $\gamma$  (INF- $\gamma$ ; 10 ng/ml, 16 h) on plates coated with fibronectin (50  $\mu\text{g/ml}$ ) at 15 min after cell seeding. Square boxes show high magnification images of the attached cells. Scale bar, 50  $\mu\text{m}$ . \*\*,  $p < 0.01$ .

**Formation of Ninjurin1-induced Membrane Protrusions Requires Rac1 Activation**—Because Ninjurin1 mediates basal cell motility by enhancing membrane protrusions, exploration of the mechanism underlying Ninjurin1-regulated membrane dynamics is warranted. The Rho family of small GTPases, RhoA, Rac1, and Cdc42, regulates cytoskeletal rearrangements that are associated with morphological transformations such as the formation of lamellipodia and filopodia (23, 24). Considerable evidence shows that the Rho family of GTPases is also involved in leukocyte trafficking (25). Therefore, we examined the basal activity of these small GTPases in *siNinj1* Raw264.7 cells. Rac activity was selectively reduced in *siNinj1* Raw264.7 cells, whereas the levels of RhoA and Cdc42 activity were similar to that in the *siCont* Raw264.7 cells (Fig. 7A). Therefore, Rac activity might regulate membrane protrusion formation downstream of Ninjurin1. We used NSC23766, a Rac1-specific inhibitor (26), to support this hypothesis. In GFP-mNinj1 Raw264.7 cells, treatment with this inhibitor significantly reduced the number of Fascin1-positive filopodial protrusions. In GFP Raw264.7 cells, the number of filopodia was slightly decreased in the presence of the inhibitor; however, no significant differ-

ence was observed between the treated and nontreated groups (Fig. 7, B and C). Taken together, Rac1 activation is required for Ninjurin1-mediated formation of filopodial membrane protrusions.

**Ninjurin1 Promotes the Formation of Adhesive and Invasive Protrusions on an Endothelial Cell Monolayer**—We previously found that Ninjurin1 regulates the TEM of immune cells across endothelial cell monolayers (17). In a previous study using transwell assays, we found that Ninjurin1-deficient BMDMs and *siNinj1* Raw264.7 cells show a decrease in their TEM activity across an MBEC4 endothelial monolayer, whereas GFP-mNinj1 Raw264.7 cells show an increase in such activity (17). These results imply a functional relationship between Ninjurin1-mediated protrusion formation and TEM. We therefore examined Ninjurin1 localization and protrusive activity in Raw264.7 cells transmigrating an MBEC4 monolayer. High magnification and three-dimensional Z-stack imaging allowed us to observe the distribution of Ninjurin1 in Raw264.7 cells as they passed through the MBEC4 monolayer using their adhesive and invasive membrane protrusions (Fig. 8A). Overexpressed Myc-mNinj1 proteins were localized to slender filopodial structures in

## Ninjurin1-mediated Motility in Immune Cells

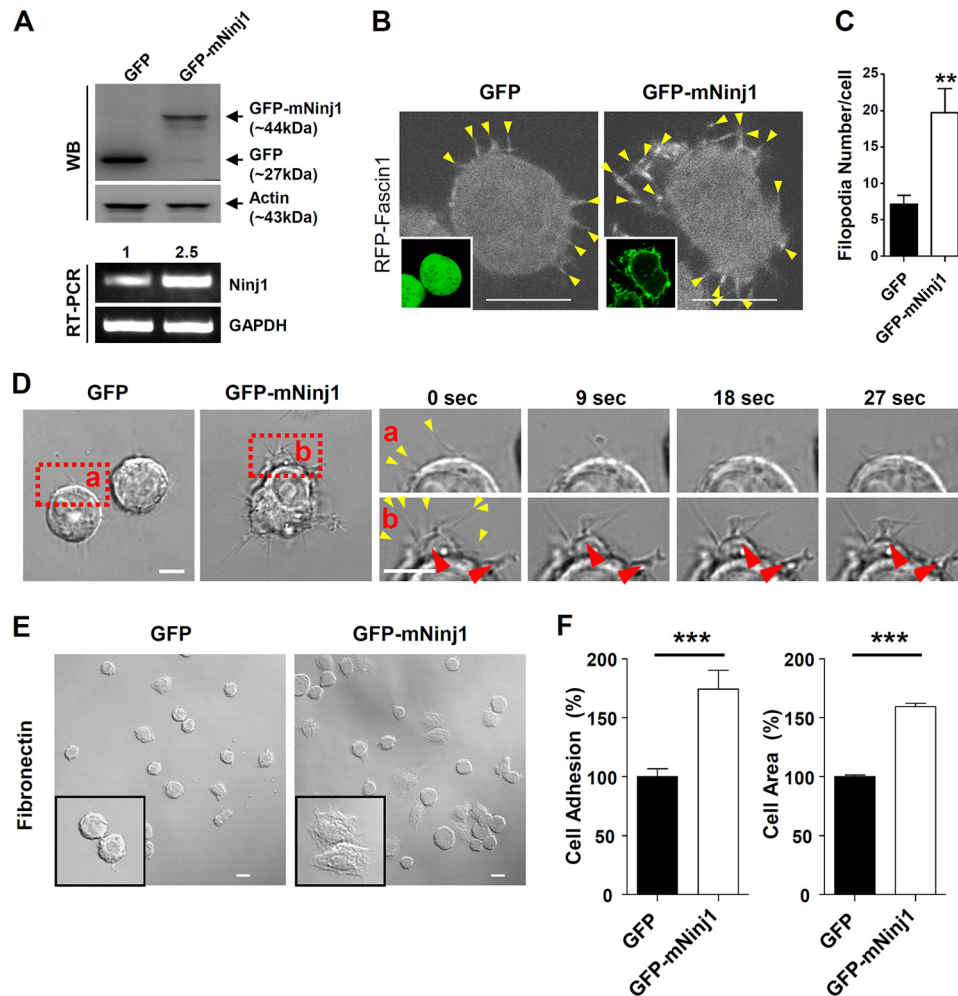


**FIGURE 5. Overexpression of Ninjurin1 in Raw264.7 cells increases the number of filopodial membrane protrusions and their dynamics.** *A*, Western blot (top panel) and RT-PCR (bottom panel) analyses of GFP and GFP-mNinj1 Raw264.7 cells. Number of RT-PCR analyses indicate relative expression of Ninjurin1 in each cell. *B* and *C*, transfection of RFP-Fascin1 into stable GFP or GFP-mNinj1 Raw264.7 cell lines. *B*, arrowheads indicate filopodial structures expressing RFP-Fascin1. Images in square boxes show the GFP signal of each cell. *C*, statistical analysis was performed using data from ~30 cells. Scale bar, 10  $\mu\text{m}$ . \*\*,  $p < 0.01$ . *D*, membrane dynamics of GFP or GFP-mNinj1 Raw264.7 cells. The red squares (panels *a* and *b*) show high magnification images of GFP and GFP-mNinj1 Raw264.7 cells, respectively. The red arrowheads indicate a pseudopodia-like foot, and the yellow arrowheads show filopodial protrusions. Scale bar, 10  $\mu\text{m}$ . *E* and *F*, adhesion and spreading of GFP and GFP-mNinj1 Raw264.7 cells on plates coated with fibronectin (50  $\mu\text{g}/\text{ml}$ ), 15 min after cell seeding. Square boxes show high magnification images of the attached cells. Scale bar, 50  $\mu\text{m}$ . \*\*\*,  $p < 0.001$ .

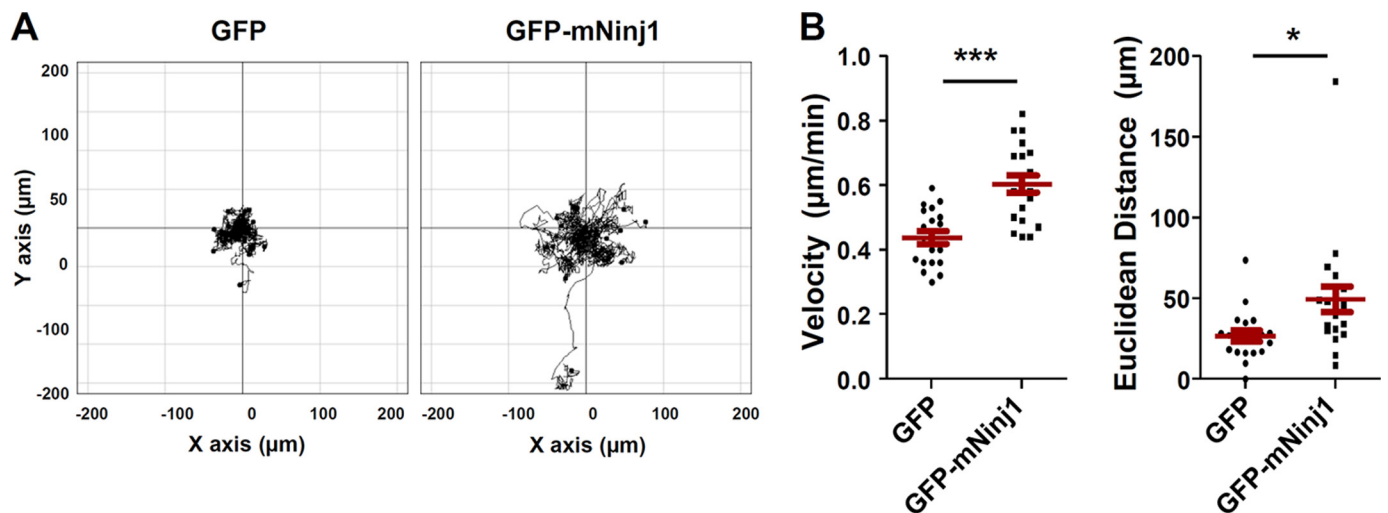


**FIGURE 6. Basal cell motility is increased in Raw264.7 cells expressing Ninjurin1.** *A* and *B*, basal motility of stable GFP and GFP-mNinj1 Raw264.7 cell lines. Phase images of stable GFP or GFP-mNinj1 Raw264.7 cells were taken every 10 min for 6 h. *A*, trajectory plot; *B*, dot charts showing the velocity and Euclidean distance of 30 cells. \*,  $p < 0.05$ ; \*\*\*,  $p < 0.001$ .

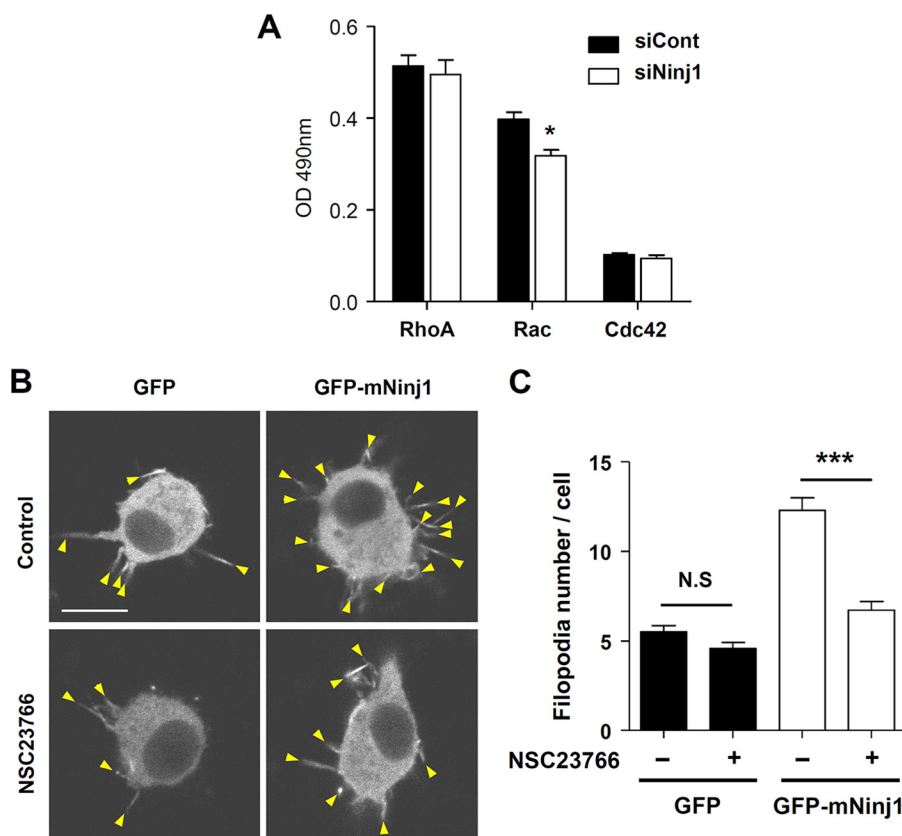


FIGURE 7. **Rac1 activation is required for Ninjurin1-mediated formation of filopodial protrusions.** *A*, analysis of the activity of small GTPases RhoA, Rac, and Cdc42 in siNinj1 by using an enzyme-linked assay. \*,  $p < 0.05$ . *B* and *C*, filopodial protrusions expressing RFP-Fascin1 (arrowheads) in GFP- or GFP-mNinj1 Raw264.7 cells after treatment with the Rac1 inhibitor NSC23766 (20  $\mu$ M, 3 h) (*B*). Representative images are shown. Arrowheads indicate filopodial structures expressing RFP-Fascin1 (*C*). The statistical analysis was performed using data from ~40 cells. Scale bar, 10  $\mu$ m. N.S., no significance; \*\*\*,  $p < 0.001$ .

the Raw264.7 cells (Fig. 8A). Furthermore, the number of the filopodial protrusions projected by GFP-mNinj1 Raw264.7 cells on the MBEC4 monolayer was greater than that of GFP cells (Fig. 8, *B* and *C*). Similarly, fewer projections were observed in siNinj1 Raw264.7 cells than in siCont cells (Fig. 8, *D* and *E*). These results suggest that Ninjurin1-mediated filopodial protrusions contribute to TEM across an endothelial monolayer.

In general, leukocytes require both motility and protrusion formation to crawl on vessel walls and transmigrate endothelial monolayers, implying that Ninjurin1-mediated protrusion formation has a role in the latter stages of leukocyte trafficking. Ninjurin1-mediated adhesion between leukocytes and the endothelium at early stages of trafficking have been well described (17, 18). Taken together with our current results, these data suggest that Ninjurin1 enhances leukocyte trafficking by performing dual stage-dependent functions, leukocyte-endothelium adhesion in the early stage, and protrusive functions during diapedesis in the later stage (Fig. 8F).

## DISCUSSION

Here, we report that Ninjurin1-mediated protrusive membrane dynamics are crucial for macrophage migration. Using cultured primary BMDMs (Figs. 1 and 2), RNAi (Fig. 4), and overexpressing Raw264.7 cells (Figs. 5 and 6) combined with time-lapse live cell imaging under high magnification, we showed that Ninjurin1 is involved in Rac1-dependent (Fig. 7) membrane protrusion formation, dynamics, cell motility, and TEM (Fig. 8).

Previously, using an EAE model, we revealed that Ninjurin1 is strongly expressed in perivascular myeloid cells and those attaching to and circulating inside the lumen of vessels. Its expression gradually decreases in leukocytes invading interstitial tissues after penetrating the EC monolayer and basement membrane (16, 17). Based on these results, we speculate that the function of Ninjurin1 is limited to leukocyte-EC interactions during extravasation rather than interstitium migration.

Leukocyte extravasation can be divided into the following five steps: attachment, rolling, adhesion, crawling, and TEM (Fig. 8F). For successful extravasation, leukocytes initially attach to the endothelium and then generate protrusive structures, podosomes (27) and filopodia (28), to penetrate the endothelial monolayer. Previous studies using neutralizing antibodies or blocking peptides showed that the adhesive activity of Ninjurin1 is important to mediate TEM (17–19). In this study, we also showed that Ninjurin1-mediated protrusive activity is involved in TEM by using Ninjurin1-deficient BMDMs, siRNA, and stable Ninjurin1-expressing cell lines. As shown in Fig. 8F, the homophilic binding activity of Ninjurin1 contributes to the rolling or adhesion of leukocytes during the initial stage when they bind to the endothelium during TEM. After the initial adhesion, Ninjurin1 plays an additional role in generating invasive membrane protrusions during the latter stage to crawl on and transmigrate the inflamed endothelium (Fig. 8F). Numerous adhesion molecules contribute to crawling and transmigra-



## Ninjurin1-mediated Motility in Immune Cells

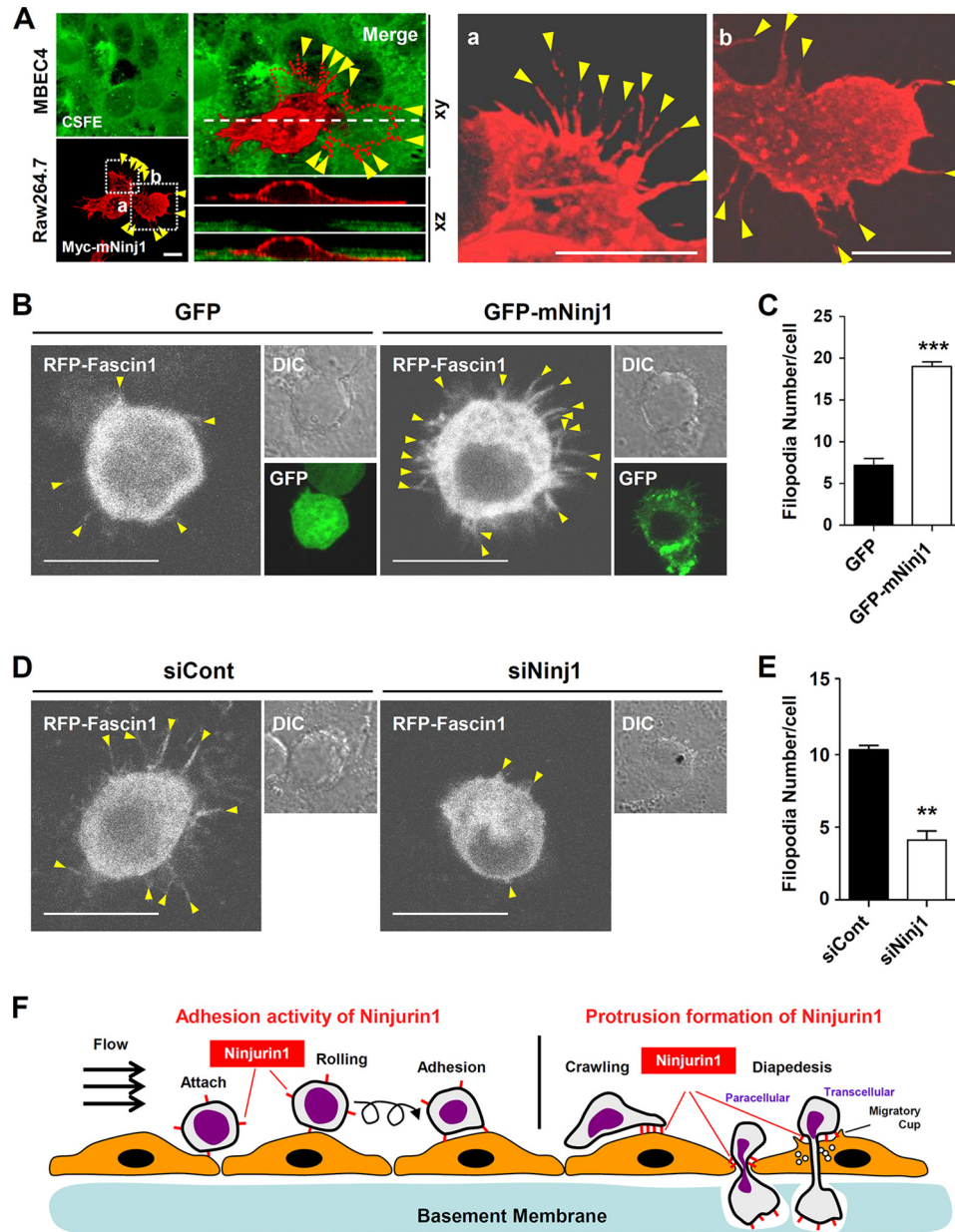


**FIGURE 8. Ninjurin1 enhances invasive filopodial protrusions used to cross MBEC4 monolayers.** *A*, Myc-mNinjur1 Raw264.7 cells (red) were plated onto a 5  $\mu\text{M}$  carboxyfluorescein diacetate succinimidyl ester (CFSE)-labeled MBEC4 monolayer (green) for 20 min, and Z-stack images were obtained. The red dotted line (left) denotes the bottom boundary of the Raw264.7 cells penetrating the MBEC4 monolayer. The white dashed line shows the region used for the Z-stack imaging. Yellow arrowheads indicate filopodial protrusion. Scale bar, 10  $\mu\text{m}$ . *B* and *C*, protrusive properties of stable GFP and GFP-mNinjur1 Raw264.7 cell lines on a MBEC4 monolayer that had been stimulated with 10 ng/ml tumor necrosis factor  $\alpha$  (TNF $\alpha$ ) and 10 ng/ml interferon- $\gamma$  (INF- $\gamma$ ) for 16 h. *B*, yellow arrowheads indicate filopodial membrane protrusions expressing RFP-Fascin1. Scale bar, 10  $\mu\text{m}$ . *C*, statistical analysis was performed using  $\sim 30$  cells per group. \*\*\*,  $p < 0.001$ . *D* and *E*, protrusive properties of siCont or siNinjur1 Raw264.7 cells on MBEC4 monolayers. *D*, yellow arrowheads indicate filopodial membrane protrusions. Scale bar, 10  $\mu\text{m}$ . *E*, statistical analysis was performed using  $\sim 30$  cells per group. \*\*,  $p < 0.01$ . *F*, schematic illustration of the stage-specific contribution of Ninjurin1 to the transmigration of leukocytes across the endothelium.

tion (1, 29, 30), and indeed, Ninjurin1-mediated adhesion participates in T cell crawling (19). Whether Ninjurin1-mediated adhesion and protrusive activities are independent or coordinated sequential processes requires further investigation.

How can Ninjurin1 regulate the Rho GTPase family to contribute to membrane protrusion formation? According to our results, Ninjurin1 drives the formation of membrane protrusions in a Rac1-dependent manner. Because Ninjurin1 is a transmembrane molecule containing a small cytoplasmic domain, it is difficult to conceive how it might interact and

regulate the activation of Rac1. Unfortunately, the upstream and downstream components that regulate Ninjurin1, such as binding partners and subcellular signaling molecules, are largely unknown. We propose that Ninjurin1 interacts with the integrin family. As an extracellular receptor, Ninjurin1 might regulate membrane surface protein clusters to activate intracellular signaling. Specialized domains in the plasma membrane, tetraspanin-enriched microdomains, act as a functional platform to support various protein-protein and protein-lipid interactions and mediate cellular events such as cell migration

and intercellular adhesion (31–33). Many transmembrane adhesion molecules such as integrins, ICAM-1, and VCAM-1 cluster in these domains, transducing subcellular signals through adaptor proteins and members of the Rho GTPase family. Therefore, we propose that Ninjurin1 interacts with other adhesion receptors or transmembrane proteins as a component of tetraspanin-enriched domains, thereby mediating Rac1 activation, the formation of protrusions, and cell migration.

We previously demonstrated that Ninjurin1 is expressed in endothelial cells and is up-regulated during inflammatory conditions *in vitro* and in the EAE spinal cord *in vivo* (16). In response to protrusion formation in leukocytes, endothelial cells generate docking structures composed of microvilli-like protrusions that are oriented toward the penetrating leukocytes and embrace them in what is termed the “migratory cup” or “podoprint” (34). Mass spectrometry proteomic screening showed Ninjurin1 is localized to lipid raft membrane microdomains isolated from human brain endothelial cells (35) that together co-localize with the migratory cup (34). These data strongly suggest that Ninjurin1 has a role in the endothelium. Whether Ninjurin1 is involved in the formation of protrusive migratory cups in endothelial cells and the mechanism underlying its interaction at the leukocyte-endothelium synapse to regulate leukocyte diapedesis are interesting subjects to address in future studies.

The involvement of Ninjurin1 in MS has been suggested on the basis of studies examining brains from patients with MS (18), MS model EAE mice (16, 18), and in mice genetically deficient in Ninjurin1 (17). Therapeutic trials using blocking antibodies and peptides to inhibit Ninjurin1 function show that Ninjurin1 is a potential target for modulating inflammatory diseases, MS in particular (18, 19). Further in-depth investigations into the properties of Ninjurin1-expressing immune cells and its adhesive activity are warranted. Here, we described a basal function of Ninjurin1 in immune cell motility. It localized with the filopodial protrusions and activated Rac1, leading to dynamic protrusive behavior. These findings provided additional insights into the understanding of Ninjurin1-mediated inflammation, promising successful and safe clinical translation of Ninjurin1-targeted therapeutics for inflammatory diseases.

## REFERENCES

- Ley, K., Laudanna, C., Cybulsky, M. I., and Nourshargh, S. (2007) Getting to the site of inflammation: the leukocyte adhesion cascade updated. *Nat. Rev. Immunol.* **7**, 678–689
- Nourshargh, S., Hordijk, P. L., and Sixt, M. (2010) Breaching multiple barriers: leukocyte motility through venular walls and the interstitium. *Nat. Rev. Mol. Cell Biol.* **11**, 366–378
- Shi, C., and Pamer, E. G. (2011) Monocyte recruitment during infection and inflammation. *Nat. Rev. Immunol.* **11**, 762–774
- Mackay, C. R. (2008) Moving targets: cell migration inhibitors as new anti-inflammatory therapies. *Nat. Immunol.* **9**, 988–998
- Lämmermann, T., Bader, B. L., Monkley, S. J., Worbs, T., Wedlich-Söldner, R., Hirsch, K., Keller, M., Förster, R., Critchley, D. R., Fässler, R., and Sixt, M. (2008) Rapid leukocyte migration by integrin-independent flowing and squeezing. *Nature* **453**, 51–55
- Friedl, P., and Weigelin, B. (2008) Interstitial leukocyte migration and immune function. *Nat. Immunol.* **9**, 960–969

- Ridley, A. J. (2011) Life at the leading edge. *Cell* **145**, 1012–1022
- Calle, Y., Burns, S., Thrasher, A. J., and Jones, G. E. (2006) The leukocyte podosome. *Eur. J. Cell Biol.* **85**, 151–157
- Mattila, P. K., and Lappalainen, P. (2008) Filopodia: molecular architecture and cellular functions. *Nat. Rev. Mol. Cell Biol.* **9**, 446–454
- Ridley, A. J., Schwartz, M. A., Burridge, K., Firtel, R. A., Ginsberg, M. H., Borisy, G., Parsons, J. T., and Horwitz, A. R. (2003) Cell migration: integrating signals from front to back. *Science* **302**, 1704–1709
- Parsons, J. T., Horwitz, A. R., and Schwartz, M. A. (2010) Cell adhesion: integrating cytoskeletal dynamics and cellular tension. *Nat. Rev. Mol. Cell Biol.* **11**, 633–643
- Nobes, C. D., and Hall, A. (1995) Rho, rac, and cdc42 GTPases regulate the assembly of multimolecular focal complexes associated with actin stress fibers, lamellipodia, and filopodia. *Cell* **81**, 53–62
- Iden, S., and Collard, J. G. (2008) Crosstalk between small GTPases and polarity proteins in cell polarization. *Nat. Rev. Mol. Cell Biol.* **9**, 846–859
- Araki, T., and Milbrandt, J. (1996) Ninjurin, a novel adhesion molecule, is induced by nerve injury and promotes axonal growth. *Neuron* **17**, 353–361
- Araki, T., Zimonjic, D. B., Popescu, N. C., and Milbrandt, J. (1997) Mechanism of homophilic binding mediated by ninjurin, a novel widely expressed adhesion molecule. *J. Biol. Chem.* **272**, 21373–21380
- Ahn, B. J., Lee, H. J., Shin, M. W., Choi, J. H., Jeong, J. W., and Kim, K. W. (2009) Ninjurin1 is expressed in myeloid cells and mediates endothelium adhesion in the brains of EAE rats. *Biochem. Biophys. Res. Commun.* **387**, 321–325
- Ahn, B. J., Lee, H., Shin, M. W., Bae, S. J., Lee, E. J., Wee, H. J., Cha, J. H., Lee, H. J., Lee, H. S., Kim, J. H., Kim, C. Y., Seo, J. H., Lo, E. H., Jeon, S., Lee, M. N., Oh, G. T., Yin, G. N., Ryu, J. K., Suh, J. K., and Kim, K. W. (2014) Ninjurin1 deficiency attenuates susceptibility of experimental autoimmune encephalomyelitis in mice. *J. Biol. Chem.* **289**, 3328–3338
- Ifergan, I., Kebir, H., Terouz, S., Alvarez, J. I., Lécuyer, M. A., Gendron, S., Bourbonnière, L., Dunay, I. R., Bouthillier, A., Moumdjian, R., Fontana, A., Haqqani, A., Klopstein, A., Prinz, M., López-Vales, R., Birchler, T., and Prat, A. (2011) Role of Ninjurin-1 in the migration of myeloid cells to central nervous system inflammatory lesions. *Ann. Neurol.* **70**, 751–763
- Odoardi, F., Sie, C., Strey, K., Ulaganathan, V. K., Schläger, C., Lodygin, D., Heckelsmiller, K., Niefeld, W., Ellwart, J., Klinkert, W. E., Lottaz, C., Nosov, M., Brinkmann, V., Spang, R., Lehrach, H., Vingron, M., Wekerle, H., Flügel-Koch, C., and Flügel, A. (2012) T cells become licensed in the lung to enter the central nervous system. *Nature* **488**, 675–679
- Ahn, B. J., Lee, H., Shin, M. W., Bae, S. J., Lee, E. J., Wee, H. J., Cha, J. H., Park, J. H., Lee, H. S., Lee, H. J., Jung, H., Park, Z. Y., Park, S. H., Han, B. W., Seo, J. H., Lo, E. H., and Kim, K. W. (2012) The N-terminal ectodomain of Ninjurin1 liberated by MMP9 has chemotactic activity. *Biochem. Biophys. Res. Commun.* **428**, 438–444
- Lee, H. J., Ahn, B. J., Shin, M. W., Jeong, J. W., Kim, J. H., and Kim, K. W. (2009) Ninjurin1 mediates macrophage-induced programmed cell death during early ocular development. *Cell Death Differ.* **16**, 1395–1407
- Quast, T., Eppler, F., Semmling, V., Schild, C., Homsy, Y., Levy, S., Lang, T., Kurts, C., and Kolanus, W. (2011) CD81 is essential for the formation of membrane protrusions and regulates Rac1-activation in adhesion-dependent immune cell migration. *Blood* **118**, 1818–1827
- Heasman, S. J., and Ridley, A. J. (2008) Mammalian Rho GTPases: new insights into their functions from *in vivo* studies. *Nat. Rev. Mol. Cell Biol.* **9**, 690–701
- Krugmann, S., Jordens, I., Gevaert, K., Driessens, M., Vandekerckhove, J., and Hall, A. (2001) Cdc42 induces filopodia by promoting the formation of an IRSp53:Mena complex. *Curr. Biol.* **11**, 1645–1655
- Cernuda-Morollón, E., and Ridley, A. J. (2006) Rho GTPases and leukocyte adhesion receptor expression and function in endothelial cells. *Circ. Res.* **98**, 757–767
- Gao, Y., Dickerson, J. B., Guo, F., Zheng, J., and Zheng, Y. (2004) Rational design and characterization of a Rac GTPase-specific small molecule inhibitor. *Proc. Natl. Acad. Sci. U.S.A.* **101**, 7618–7623
- Carman, C. V., Sage, P. T., Sciuto, T. E., de la Fuente, M. A., Geha, R. S., Ochs, H. D., Dvorak, H. F., Dvorak, A. M., and Springer, T. A. (2007) Transcellular diapedesis is initiated by invasive podosomes. *Immunity* **26**,

## Ninjurin1-mediated Motility in Immune Cells

784–797

28. Shulman, Z., Shinder, V., Klein, E., Grabovsky, V., Yeger, O., Geron, E., Montresor, A., Bolomini-Vittori, M., Feigelson, S. W., Kirchhausen, T., Laudanna, C., Shakhar, G., and Alon, R. (2009) Lymphocyte crawling and transendothelial migration require chemokine triggering of high-affinity LFA-1 integrin. *Immunity* **30**, 384–396
29. Schenkel, A. R., Mamdouh, Z., and Muller, W. A. (2004) Locomotion of monocytes on endothelium is a critical step during extravasation. *Nat. Immunol.* **5**, 393–400
30. Imhof, B. A., and Aurrand-Lions, M. (2004) Adhesion mechanisms regulating the migration of monocytes. *Nat. Rev. Immunol.* **4**, 432–444
31. Barreiro, O., Yáñez-Mó, M., Sala-Valdés, M., Gutiérrez-López, M. D., Ovalle, S., Higginbottom, A., Monk, P. N., Cabañas, C., and Sánchez-Madrid, F. (2005) Endothelial tetraspanin microdomains regulate leukocyte firm adhesion during extravasation. *Blood* **105**, 2852–2861
32. Ley, K., and Zhang, H. (2008) Dances with leukocytes: how tetraspanin-enriched microdomains assemble to form endothelial adhesive platforms. *J. Cell Biol.* **183**, 375–376
33. Barreiro, O., Zamai, M., Yáñez-Mó, M., Tejera, E., López-Romero, P., Monk, P. N., Gratton, E., Caiolfa, V. R., and Sánchez-Madrid, F. (2008) Endothelial adhesion receptors are recruited to adherent leukocytes by inclusion in preformed tetraspanin nanoplateforms. *J. Cell Biol.* **183**, 527–542
34. Carman, C. V., and Springer, T. A. (2004) A transmigratory cup in leukocyte diapedesis both through individual vascular endothelial cells and between them. *J. Cell Biol.* **167**, 377–388
35. Dodelet-Devillers, A., Cayrol, R., van Horssen, J., Haqqani, A. S., de Vries, H. E., Engelhardt, B., Greenwood, J., and Prat, A. (2009) Functions of lipid raft membrane microdomains at the blood-brain barrier. *J. Mol. Med.* **87**, 765–774